

## PHONON SPECTROSCOPY OF ORIENTED HCP IRON

H. GIEFERS<sup>a</sup>, R. LÜBBERS<sup>a</sup>, K. RUPPRECHT<sup>a</sup>, G. WORTMANN<sup>a,\*</sup>,  
D. ALFÈ<sup>b</sup> and A. I. CHUMAKOV<sup>c</sup>

<sup>a</sup>Fachbereich Physik, University of Paderborn, D-33095 Paderborn, Germany; <sup>b</sup>University College London, London WC1E 6BT, UK; <sup>c</sup>ESRF, Experimental Division, BP 220, F-38043 Grenoble, France

(Received 19 July 2001; In final form 28 September 2001)

High-pressure phonon spectroscopy was performed on iron in the bcc and hcp phase up to 40 GPa using the nuclear inelastic scattering (NIS) of synchrotron radiation (SR). In hcp iron we observe differences in the density of phonon states for spectra measured with different orientations of the diamond anvil cell (DAC) with respect to the SR beam. These differences are attributed to a preferred orientation of the hexagonal *c*-axis along the load axis of the DAC. These texture effects are used, in conjunction with theoretical calculations, to extract density of phonon states as seen parallel and perpendicular to the *c*-axis of hcp iron.

*Keywords:* Phonon density of states, bcc iron, hcp iron, high pressure

### INTRODUCTION

The hexagonal (hcp) high-pressure phase of iron,  $\epsilon$ -Fe, is the most relevant phase of the Earth's inner core and the thermodynamic and elastic properties at core conditions are of actual geophysical interest [1]. This holds especially for the sound velocities, since seismic wave experiments deliver almost exclusively information from the core [1]. At ambient pressure and temperature, iron is magnetic and crystallizes in the cubic (bcc) structure ( $\alpha$ -Fe). Around 13 GPa,  $\alpha$ -Fe transforms to the nonmagnetic  $\epsilon$ -Fe. High-pressure (h.p.) experiments with synchrotron radiation from 3rd generation sources like the European Synchrotron Radiation Facility (ESRF, Grenoble) and the Advanced Photon Source (APS, Argonne) have contributed in the last few years considerably to the knowledge of the *p*, *T* phase diagram and other properties of iron at conditions approaching the Earth's core [2–6].

The new technique of Nuclear Inelastic Scattering (NIS), introduced in 1995 and especially suited to measure phonon density-of-states (DOS) at Mössbauer nuclei like Fe-57 [7–9], was recently applied to measure, for the first time, the phonon density-of-states (DOS) in  $\epsilon$ -Fe up to 42 GPa at the ESRF [4] and up to 153 GPa at the APS [5]. NIS studies benefit from the fact that the phonon DOS can be measured from a polycrystalline sample. This is different to the conventional way of determining phonon DOS by inelastic neutron

---

\* Corresponding author. Fax: +49-5251-603216; E-mail: wo-gw@physik.upb.de

scattering, where single crystals are needed to measure the dispersion relations, as described in a recent neutron scattering study of a single crystal of  $\alpha$ -Fe up to 10 GPa [10]. Because of the need of single crystals, inelastic neutron scattering is limited to systems, where these single crystals can be grown at ambient pressure.

In this contribution we demonstrate that, by using the pressure-induced texture in our samples, we can produce phonon DOS spectra corresponding to those measured from a single-crystalline  $\varepsilon$ -Fe sample parallel or perpendicular to the  $c$ -axis. This enables us to attribute characteristic spectral features to specific phonon modes, which facilitates direct comparison with theoretical calculations [11, 12] and other spectroscopic methods [13, 14].

## EXPERIMENTAL

Fe-57 NIS experiments of  $\alpha$ -Fe and  $\varepsilon$ -Fe at pressures up to 40 GPa were performed with an improved experimental set-up at the beamline ID22N of ESRF ([see Ref. 4]). A high-resolution monochromator with two pairs of channelcut Si(3 3 3) and Si(9 7 5) crystals provided an energy resolution of 3.9 meV for the 14.413 keV transition of Fe-57, in comparison to about 6 meV in the previous study [4]. By the use of compound refractive lenses and a bent crystal the monochromatized beam was focused to a size of  $90\ \mu\text{m} \times 60\ \mu\text{m}$  ( $h \times v$ ) with  $3 \times 10^8$  photons/s at 90 mA storage ring current. We have modified our h.p. cells by two additional openings allowing now also NIS studies with the SR beam both along and almost perpendicular (at an angle of  $70^\circ$ – $90^\circ$ ) to the diamond anvil axis (see Fig. 1). This modification of the h.p. cell enabled us to study the impact of a preferred orientation on the phonon DOS. It is known that  $\varepsilon$ -Fe orients, after the bcc-hcp transition around 13 GPa, with the  $c$ -axis preferentially parallel to the load axis [2, 3].

## EXPERIMENTAL RESULTS

Fe-57 NIS spectra were recorded for  $\alpha$ -Fe (bcc) at ambient pressure and at 6.9 GPa as well as for  $\varepsilon$ -Fe (hcp) at 28 GPa and 40 GPa. Normalized NIS spectra of  $\alpha$ -Fe at ambient pressure and

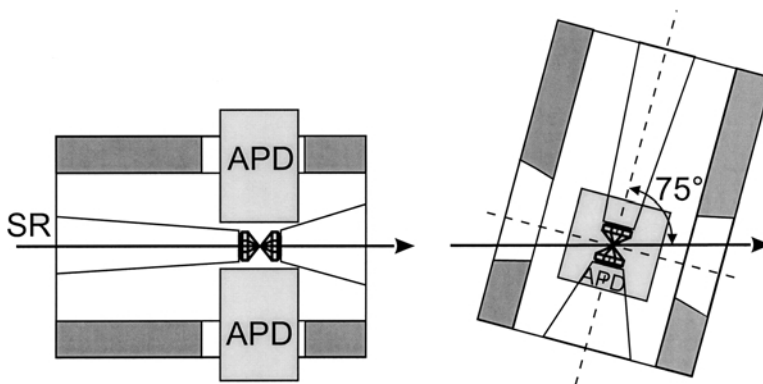


FIGURE 1 Sketch of the h.p. cell at two different orientations ( $0^\circ$  and  $75^\circ$ ) with respect to the SR beam. The iron sample is contained in a Be gasket between the two diamonds. This gasket material allows sufficient transmission of the 6.4 and 7.0 keV  $K_{\alpha,\beta}$  X-ray fluorescence following with 90% after the resonant excitation of the 14.413 keV level of Fe-57 [4, 5]. The avalanche photo diodes (APD) serve for the detection of the Fe  $K_{\alpha,\beta}$  fluorescence.

of  $\varepsilon$ -Fe at 40 GPa are shown in Figure 2, where the right-hand wing reflects the creation of phonons and the left-hand wing reflects the annihilation of phonons. The spectra exhibit drastic differences due to (i) the different structures and (ii) the different binding strength, the latter expressed by the Debye temperature,  $\Theta_D$ . In the normalized NIS spectra the area under the inelastic side wings scales with  $1 - f_{LM}$ , where  $f_{LM}$  is the Lamb-Mössbauer factor for elastic (recoil-free) scattering of the gamma radiation [8, 9].

The phonon DOS of  $\alpha$ -Fe and  $\varepsilon$ -Fe at various pressures, derived from the measured NIS spectra by subtraction of multi-phonon excitations and by the elastic line [8, 9], are shown in Figure 3. They exhibit characteristic spectral features (peaks) for the  $\alpha$ - and  $\varepsilon$ -phase with clear pressure-induced shifts of these peak to higher energy. The present data for  $\alpha$ -Fe agree well with recent neutron data, the shift of the characteristic spectral feature, the sharp peak in the phonon DOS, from 36 meV to 38.5 meV (0 to 6.9 GPa) compares well with that derived in the neutron study from 36 meV to 39 meV (0 to 9.8 GPa) [10]. For the  $\alpha$ -Fe spectra we observe, within statistical accuracy, no difference between the spectra measured at different orientations of the h.p. cell with respect to the beam. The phonon DOS spectra can be used [8, 9] to derive the thermodynamic and elastic parameters for  $\alpha$ -Fe and  $\varepsilon$ -Fe at various pressures. From the derived Debye temperatures we obtain for  $\alpha$ -Fe a Grüneisen parameter,  $\gamma = -d \ln \theta_D / d \ln V = 2.0(0.2)$ , in good agreement with  $\gamma = 1.9(2)$  derived from the neutron data [10].

In the case of  $\varepsilon$ -Fe, systematic differences were observed for the two orientations,  $0^\circ$  and  $75^\circ$ , of the h.p. cell with respect to the beam (see Fig. 1). This indicates the existence of a preferred orientation in the  $\varepsilon$ -Fe sample with implications on the phonon spectra. The derived thermodynamic and elastic parameters for  $\varepsilon$ -Fe are will be discussed later. It should be mentioned that the present data for  $\varepsilon$ -Fe are, due to the enhanced resolution, more precise than those in Ref. [4] and agree well with those in Ref. [5].

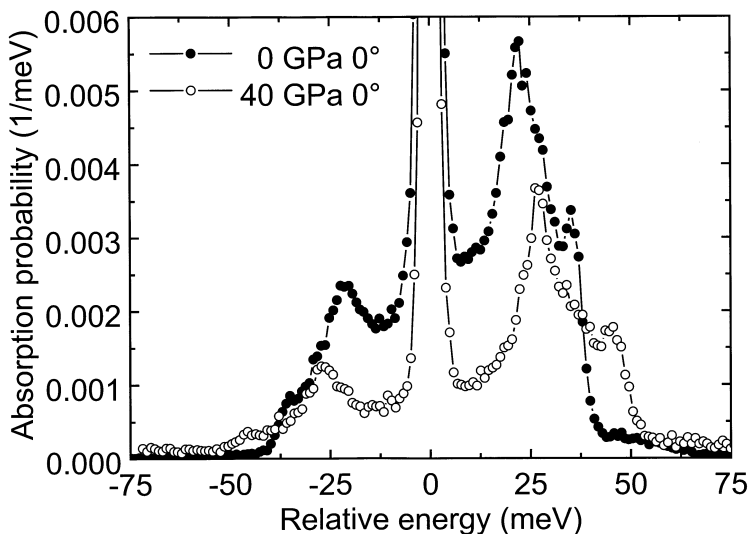


FIGURE 2 Nuclear inelastic scattering (NIS) spectra of Fe at ambient pressure ( $\alpha$ -Fe, full dots) and at 40 GPa ( $\varepsilon$ -Fe, open dots). The spectra are shown after normalisation according to the procedure in [8, 9]. The intensity of the inelastic part (sidebands) decreases by about 50% between 0 and 40 GPa, reflecting the change in  $f_{LM}$  from about 0.8 to 0.9.

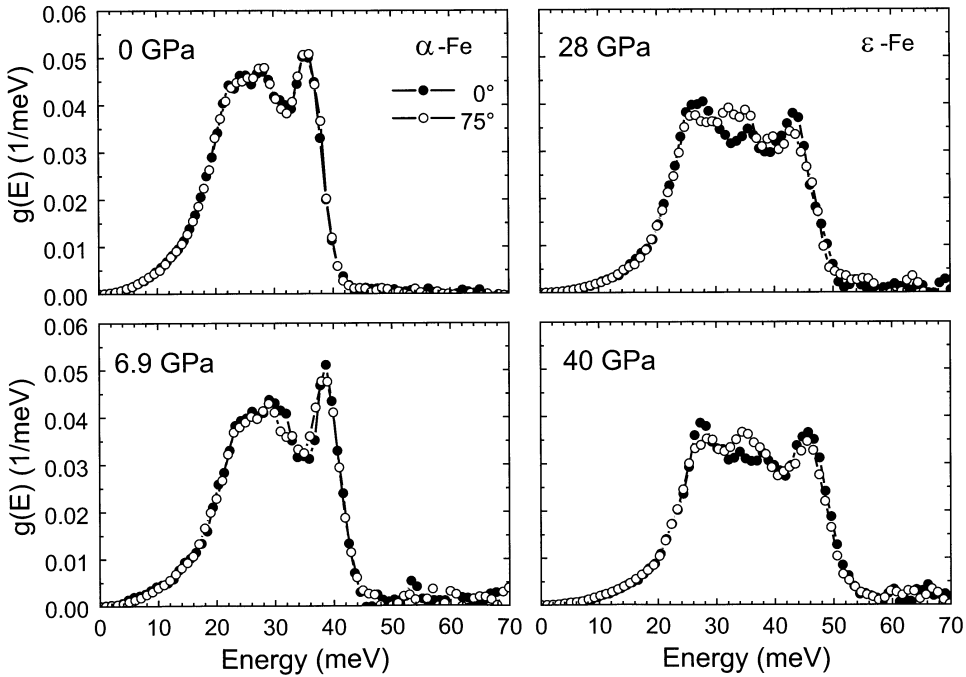


FIGURE 3 Density of phonon states  $g(E)$  of  $\alpha$ -Fe and  $\epsilon$ -Fe at various pressures. Full dots correspond to measurements performed at an angle of  $0^\circ$  between the SR beam and the axis of the diamonds, open dots to measurements performed at an angle  $75^\circ$ .

### TEXTURE IN HCP IRON: THEORETICAL CALCULATIONS VERSUS EXPERIMENTAL RESULTS

In order to explain the dependence of the observed phonon DOS on the orientation of the h.p. cell, theoretical calculations of the phonon dispersion relations and phonon-DOS were performed for  $\epsilon$ -Fe with an *ab-initio* method described in [5, 11]. Dispersion relations for different directions in the Brillouin zone of the hcp lattice were calculated with the lattice parameters of  $\epsilon$ -Fe at 40 GPa. The dispersion relations were used to derive the integral phonon DOS as well as projected DOS as seen along the  $c$ -axis and within the  $a$ ,  $b$ -plane perpendicular the  $c$ -axis are shown in Figure 4 (details of these calculations will be published elsewhere [17]). The projected phonon DOS along the  $c$ -axis exhibits two sharp features of the two optical phonon branches at the  $\Gamma$  point of the Brillouin zone; the projected DOS of the  $a$ ,  $b$ -plane exhibit a multi-peaked structure with dominant contributions with a maximum around 38 meV.

The probability of inelastic nuclear absorption varies with  $\cos^2\vartheta$ , where  $\vartheta$  is the angle between the  $k$ -vector of the incident synchrotron radiation and the polarization vector of the excited or annihilated phonon [8, 15], as proved by NIS studies of single crystalline samples [15, 16]. Assuming a preferred orientation of the  $c$ -axis along the diamond axis, then the theoretical DOS as displayed in Figure 5b should be enhanced and the one perpendicular to the  $c$ -axis (Fig. 5c) should be diminished when the NIS spectra are measured along the diamond anvil axis ( $0^\circ$  spectra). When measured at  $75^\circ$  with respect to the diamond axes, just the opposite should happen. Other crystallographic directions, *e.g.* the  $(1, 0, 1)$  direction, should vary much less, since they are less influenced by a texture of the  $c$ -axis as visualized

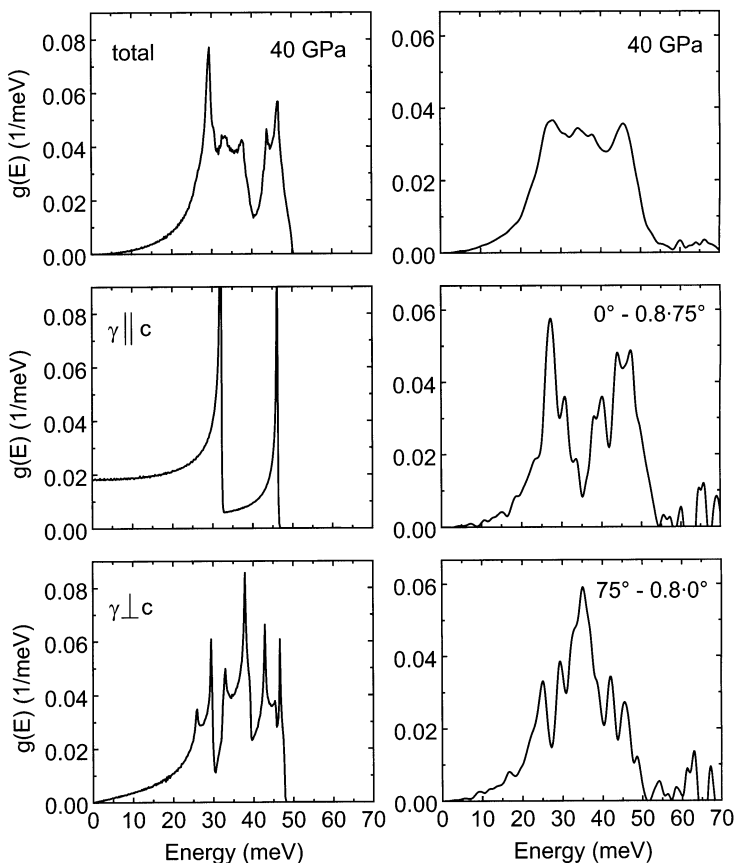


FIGURE 4 (left column): Theoretical phonon DOS of  $\epsilon$ -Fe at 40 GPa. (a) total phonon DOS for a polycrystalline sample, (b) projection of the DOS along the  $c$ -axis and (c) perpendicular to the  $c$ -axis. Due to the van Hove singularity of the optical modes, the DOS seen parallel to the  $c$ -axis could not be normalized in (b). (right column): Experimental phonon DOS of  $\epsilon$ -Fe (a) from addition of the normalized phonon DOS measured at  $0^\circ$  and  $75^\circ$  (see Fig. 3), (b) phonon DOS as obtained from the  $0^\circ$  DOS spectrum after subtraction of 80% of the  $75^\circ$  DOS spectrum, (c) phonon DOS as obtained from the  $75^\circ$  DOS spectrum after subtraction of 80% of the  $0^\circ$  DOS spectrum.

from the corresponding peaks in the XRD spectra [3]. It will be shown elsewhere [17] that texture effects can be reduced or enhanced by subtracting appropriate amounts of the normalized DOS spectra observed at  $0^\circ$  and  $75^\circ$ . Figure 4 (right column) shows such added and subtracted DOS spectra. Considering the experimental spectral resolution of 3.9 meV, there is very good agreement in the characteristic spectral features between the theoretical DOS and the added/subtracted experimental DOS spectra.

With this information we attribute the peaks at 27 (28) meV and 44 (46) meV in the 28 (40) GPa DOS spectra to the optical modes seen along the  $c$ -axis. This interpretation is supported by recent Raman studies of  $\epsilon$ -Fe [13, 14], where the Raman active  $E_{2g}$  mode was observed at frequencies of  $215 \text{ cm}^{-1}$  (28 GPa) and  $225 \text{ cm}^{-1}$  (40 GPa), which corresponds exactly to the maxima at lower energy in the measured phonon DOS.

The derived thermodynamic and elastic parameters of  $\epsilon$ -Fe can be used to look for an anisotropy with respect to the  $c$ -axis. It may be reminded that the observed anisotropy in the sound velocities of the Earth's inner core were speculatively attributed to a highly textured  $\epsilon$ -Fe core [18, 19]. The present values for the average sound velocities  $v_D$ , derived from

the slope of the phonon DOS in the low energy range from 0 to 15 meV [4], with  $v_D = 4.38(6)$  and  $4.39(6)$  km/s at 28 GPa and  $v_D = 4.59(6)$  and  $4.47(6)$  km/s at  $0^\circ$  and  $75^\circ$ , respectively, indicate within the error bars no differences for the two directions. The same holds for the derived Debye temperatures with average values of  $\Theta_D = 511(3)$  K and  $543(3)$  K at 28 and 40 GPa, respectively. Finally, the derived Grüneisen parameter for  $\varepsilon$ -Fe,  $\gamma = 1.8(2)$ , compares well with  $\gamma = 1.68(20)$  from the Raman study [13] and with  $\gamma = 1.78(6)$  from the XRD study [2].

Future NIS studies on highly-textured  $\varepsilon$ -Fe samples, performed at higher pressures and higher statistical accuracy, may allow to answer the question about anisotropic properties of  $\varepsilon$ -Fe with implications for the Earth's core.

### **Acknowledgement**

We thank Bryan Doyle, Olaf Leupold, Rudolf Rüffer for their friendly help with the experiments at ESRF. We acknowledge useful discussions with Wolfgang Sturhahn. This work was supported by the BMBF (05 SK8PPA 0).

### **References**

- [1] Mao, H.-K. and Hemley, R. J. (1998). In: *Ultra-high Pressure Mineralogy; Physics and Chemistry of the Earth's Deep Interior*. Mineralogical Society of America, Washington, DC.
- [2] Dubrovinsky, L. S., *et al.* (2000). *Phys. Rev. Lett.*, **84**, 1720; see also ESRF Highlights 1999, p. 73.
- [3] Wenk, H.-R., *et al.* (2000). *Nature*, **405**, 1044.
- [4] Lübbers, R., Grünsteudel, H. F., Chumakov, A. I. and Wortmann, G. (2000). *Science*, **287**, 1250.
- [5] Mao, H.-K., *et al.* (2001). *Science*, **292**, 914.
- [6] Fiquet, G., *et al.* (2001). *Science*, **291**, 469.
- [7] Seto, M., *et al.* (1995). *Phys. Rev. Lett.*, **74**, 3828.
- [8] Sturhahn, W., *et al.* (1995). *Phys. Rev. Lett.*, **74**, 3832.
- [9] Chumakov, A. I. and Sturhahn, W. (1999). *Hyperfine Interactions*, **123/124**, 781.
- [10] Klotz, S. and Braden, M. (2000). *Phys. Rev. Lett.*, **85**, 3209.
- [11] Alfé, D., *et al.* (1999). *Nature*, **401**, 462.
- [12] Söderlind, P., *et al.* (1996). *Phys. Rev.*, **B 53**, 14063; Steinle-Neumann, G., *et al.* (1999). *Phys. Rev. B*, **60**, 791.
- [13] Merkel, S., *et al.* (2000). *Science*, **288**, 1626.
- [14] Olijnyk, H., Jephcoat, A. P. and Refson, K. (2001). *Europhys. Lett.*, **53**, 504.
- [15] Chumakov, A. I., *et al.* (1997). *Phys. Rev. B*, **56**, 10758.
- [16] Paulsen, H., *et al.* (2001). *Phys. Rev. Lett.* **86**, 1351.
- [17] Giefers, H., *et al.*, to be published.
- [18] Stixrude, L. and Cohen, R. E. (1995). *Science*, **267**, 1972.
- [19] Creager, K. C. (1992). *Nature*, **356**, 309 and Creager, K. C. (1997). *Science*, **278**, 1284.